Research Square

Preprints are preliminary reports that have not undergone peer review.
They should not be considered conclusive, used to inform clinical practice,
or referenced by the media as validated information.

Decoding the Antimicrobial Potential of Bacillus Subtilis Onu 1125 From Deep Black Sea Sediments: An Integrated Genomic and Metabolomic Approach

Mykola Patyka
Qufu Normal University
Nataliia Vasylieva[3]
Odesa Mechnikov National University
Mykola Shtenikov[3]
Odesa Mechnikov National University
Oleksandr Andriushchenko[3]
Odesa Mechnikov National University
Iryna Strashnova[3]
Odesa Mechnikov National University
Vadym Sukmanskyi[3]
Odesa Mechnikov National University
Hennadii Lisiutin[3]
Odesa Mechnikov National University
Andrii Ostapchuk[3]
Odesa Mechnikov National University
Tetiana Ivanytsia[3]
Odesa Mechnikov National University
Mykola Galkin
kgalkin@onu.edu.ua

Odesa Mechnikov National University
Volodymyr Ivanytsia[3]
Odesa Mechnikov National University
Renjun Wang
Qufu Normal University

Article

Keywords: Bacillus subtilis, genome, exometabolome, biosynthetic gene clusters, antimicrobial exometabolites

Posted Date: October 9th, 2026

DOI: https://doi.org/10.21203/rs.3.rs-11131513/v1

License: This work is licensed under a Creative Commons Attribution 4.0 International License. Read Full License

Additional Declarations: No competing interests reported.

Abstract

Marine-derived *Bacillus* species are prolific sources of bioactive compounds with agricultural applications. Deep sediments of the Black Sea represent an underexplored ecological niche that may harbor bacterial strains with distinctive antimicrobial potential. This study aimed to evaluate the genomic and metabolomic potential of the Black Sea deep-sediment strain *Bacillus subtilis* ONU 1125 as a promising biocontrol agent against phytopathogenic microorganisms. The strain was isolated from Black Sea bottom sediments collected at 1,537 m depth. Genome annotation and biosynthetic gene cluster prediction were performed using multiple genome-mining tools, and exometabolites were profiled by HPLC-MS. The draft genome assembly of *B. subtilis* ONU 1125 comprises 4,259,067 bp, with a G + C content of 43.4% and 4,512 predicted coding sequences, including 717 hypothetical proteins. Sixteen candidate biosynthetic regions were identified, containing BGCs predicted to encode terpenes, type III polyketide synthases (T3PKS), non-ribosomal peptide synthetases (NRPS), NRP-metallophores, betalactones, glycocins, cyclodipeptide synthases (CDPS), sactipeptides, epipeptides, and ranthipeptides. Metabolomic profiling of the exometabolome revealed 20 putatively annotated metabolites, including lipopeptides, polyketides, cyclic dipeptides, a NRPS-PKS hybrid, and a phenazine-like derivative. *B. subtilis* ONU 1125 exhibits a robust genomic and metabolic arsenal, highlighting its potential for development as an effective biocontrol agent.

INTRODUCTION

The genus *Bacillus* represents one of the most diverse and ubiquitous groups of bacteria in the environment, renowned for its significant biotechnological potential stemming from the production of a wide range of bioactive secondary metabolites [1]. Within this genus, marine-derived *Bacillus* species are of particular interest for industrial and agricultural applications. They serve as prolific sources of novel metabolites with broad-spectrum biological activity, making them valuable for screening and development of innovative bioproducts [2, 3].

The bioactive secondary metabolites synthesized by marine bacilli are characterized by high structural diversity and multifaceted functions, including potent antimicrobial, antiviral, antifungal, and plant growth-promoting activities. It is well-documented that the primary antimicrobial compounds produced by these marine strains are ribosomally and non-ribosomally synthesized peptides, along with polyketides [4].

The capacity of marine-derived *Bacillus* species to produce bioactive secondary metabolites - which protect plants from pathogens, activate systemic immunity, stimulate growth, and enhance soil fertility - underpins their isolation, screening, and application as biocontrol agents for developing biological preparations [5, 6]. This approach is a core pillar of organic and ecological agriculture, which integrates innovative strategies with traditional practices to achieve high crop yields while limiting the use of synthetic fertilizers, pesticides, growth regulators, and other potentially hazardous substances [7].

Whole-genome sequencing (WGS) provides a comprehensive understanding of the metabolic and bioregulatory mechanisms of biotechnologically relevant bacteria, facilitating their broader industrial implementation. Furthermore, an integrated genomic-metabolomic approach, combining the identification of biosynthetic gene clusters (BGCs) with the profiling of metabolites in the fermentation broth, provides critical insights into the chemical structures and biosynthetic pathways of these compounds [4, 8, 9].

Previous studies established that *Bacillus subtilis* ONU 1125 isolated from the deep sediments of the Black sea (1,537 m) exhibits potent antagonistic activity against various phytopathogenic microorganisms, especially strains of *Fusarium oxysporum* [10]. These pathogens were identified as the primary agents affecting cereal crops in Southern Ukraine during the 2021–2023 period [11]. Furthermore, this strain has demonstrated plant growth-promoting (PGP) activity in cereal seedlings [12].

This study aimed to evaluate the genomic and metabolomic potential of the Black Sea deep-sediment strain *Bacillus subtilis* ONU 1125 as a promising biocontrol agent against phytopathogenic microorganisms.

RESULTS

General genomic characteristics of B. subtilis ONU 1125

The draft genome assembly of *B. subtilis* ONU 1125 comprises 11 contigs with a total length of 4,259,067 bp and a G + C content of 43.4%. The genomic analysis identified 4,512 predicted coding sequences (CDS). Among these:

- 717 genes (15.8% of all coding regions) were classified as hypothetical proteins.
- 3,795 genes (84.2%) were assigned potential functional roles.

The assembly exhibits high quality, with an estimated genome completeness of 99.8%. Furthermore, the genomic architecture includes 66 tRNA genes and three annotated rRNA features (Table 1).

Table 1
General genomic characteristics of *B. subtilis* ONU 1125

Category / Feature	Parameter	Value
Genome Statistics	Contigs	11
	Genome length	4,259,067
	GC content	43.4
	Contig L50	1
	Contig N50	2,262,045
Annotation Statistics	tRNA	66
	rRNA	3
	CDS	4,512
	CDS ratio	1,059
	Hypothetical CDS	714
	Hypothetical CDS ratio	0.369
	PLFAM CDS	4,215
	PLFAM CDS ratio	0.93
Protein Features	Hypothetical proteins	717
	Proteins with functional assignments	3,795
	Proteins with EC number assignments	1,075
	Proteins with GO assignments	896
	Proteins with pathway assignments	793
	Proteins with subsystem assignments	1,304
	Proteins with PATRIC genus-specific family (PLfam) assignments	4,215
	Proteins with PATRIC cross-genus family (PGfam) assignments	4,302
Specialty Genes	Virulence factor (PATRIC_VF)	2
	Virulence factor (Victors)	3
	Transporter (TCDB)	336
	Drug target (DrugBank)	72
	Drug target (TTD)	1
	Antibiotic resistance (PATRIC)	46
	Antibiotic resistance (CARD)	11

Category / Feature	Parameter	Value
	Antibiotic resistance (NDARO)	3

The Proksee/CGView platform was used to generate a circular representation of the draft genome assembly of *B. subtilis* ONU 1125 (Fig. 1).

Taxonomic status and phylogenetic analysis of B. subtilis ONU 1125

In previous research, strain ONU 1125 was identified as *B. subtilis* based on the characterization of its phenotypic (biological) properties and fatty acid methyl ester (FAME) profile analysis [13]. To validate species identity, elucidate phylogenetic lineages, and refine the taxonomic placement, a comprehensive suite of bioinformatics tools was utilized. Closely related strains were identified through the Type Strain Genome Server (TYGS) (https://tygs.dsmz.de/) based on whole-genome digital DNA–DNA hybridization (dDDH) analysis, as summarized in Table 2.

Table 2
In silico DNA–DNA hybridization (dDDH) values between strain B. subtilis ONU 1125 and related type strains

Reference strain	dDDH (d0, in %)	95% C.I. (%)	G + C difference (%)
Bacillus subtilis subsp. subtilis ATCC 6051^T	94.3	[91.9–96.1]	0.15
Bacillus stercoris D7XPN1	86.8	[83.2–89.7]	0.44
Bacillus spizizenii TU-B-10	82.1	[78.2–85.4]	0.47
Bacillus inaquosorum KCTC 13429	82.1	[78.2–85.4]	0.33
Bacillus rugosus SPB7	79.5	[75.5–83.0]	0.23
Bacillus cabrialesii TE3	84.2	[80.4–87.4]	0.76
Bacillus cabrialesii subsp. *tritici* TSO2	83.4	[79.4–86.4]	0.57
Bacillus tequilensis NCTC13306	64.6	[60.8–68.2]	0.62
Bacillus vallismortis DV1-F-3	66.2	[62.4–69.9]	0.4
Bacillus mexicanus FSQ1	65.3	[61.5–68.9]	0.37

Note: *d*0 (dDDH, in %) – the sum of all High-Scoring Segment Pair (HSP) lengths divided by the total genome length; C.I. – confidence intervals; ^{T} - type strain.

According to the dDDH values (Table 2) and the topology of the reconstructed phylogenetic tree (Fig. 2), *B. subtilis* ONU 1125 was identified as the phylogenetically closest strain to type strain of the species *B. subtilis* ATCC 6051^T (94.3% similarity). Genomic similarity levels with other species within the *Bacillus* genus were notably lower, ranging from 86.8% to 64.6%.

Independent identification via k-mer analysis using the KmerFinder-3.2 server further validated the assignment of the investigated strain to the *B. subtilis* species. Consequently, the comprehensive genomic evidence obtained through multiple bioinformatics tools robustly confirms that strain ONU 1125 is a representative of the species *B. subtilis*. Detailed comparative data for the closely related strains are summarized in Supplement Table S1.

Most reference strains were derived from geographically disparate terrestrial environments, in contrast to *B. subtilis* ONU 1125, which was uniquely isolated from deep-sea benthic sediments of the Black Sea (Supplement Table S1).

BGCs for secondary metabolites in the B. subtilis ONU 1125 genome

Genome mining of the *B. subtilis* ONU 1125 genome using antiSMASH version 8.0.4 (https://antismash.secondarymetabolites.org/) revealed 16 distinct regions potentially involved in the synthesis of bioactive compounds. Among the identified BGCs associated with secondary metabolism, the following types were characterized: two terpenes, two type III polyketide synthases (T3PKS), one polyketide synthase-like (PKS-like) cluster, one trans-acyltransferase polyketide synthase (trans-AT PKS), six non-ribosomal peptide synthetases (NRPS), one NRP-metallophore, one betalactone, one glycocin, one CDPS, two sactipeptides, one epipeptide, and one ranthipeptide (Table 3, Fig. 3).

Table 3
Biosynthetic gene clusters (BGCs) for secondary metabolites in the *B. subtilis* ONU 1125 genome (antiSMASH 8.0.4 analysis)

Region	Type	Cluster size (n.p.)	Most Similar Cluster (MiBIG ID)	Type of product being synthesized	Similarity (%)	The cluster is found in:
1.1	Terpene	20,798	not defined	not defined	–	–
1.2	Trans-AT PKS, PKS-like, T3PKS, NRPS	114,769	Bacillaene (BGC0002135)	Polyketide + NRP	100	*Xenorhabdus bovienii* SS-2004
1.3	NRPS, Betalactone	77,749	Fengycin (BGC0000407.5)	NRPS	100	*Bacillus subtilis subsp. subtilis*
1.4	Terpene	21,899	Not assigned	Not assigned	–	–
1.5	Glycocin	20,171	Sublancin 168 (BGC0000558.5)	RiPP: Lanthipeptide	100	*Bacillus subtilis subsp. subtilis* str. 168
1.6	T3PKS	41,098	1-carbapen-2-em-3-carboxylic acid (alkylpyrone-407 - BGC0001831.3)	Other	51	*Myxococcus xanthus*
1.7	Terpene-precursor	2,091	Not assigned	Not assigned	–	–
2.1	NRP-metallophore, NRPS	66,260	Bacillibactin (BGC0000309.5)	NRPS	100	*Bacillus subtilis subsp. subtilis* str. 168
2.2	CDPS	20,747	Pulcherriminic acid (BGC0002103.2)	Other	100	*Bacillus subtilis subsp. subtilis* str. 168
2.3	Sactipeptide	21,612	Subtilosin A (BGC0000602.5)	RiPP:Thiopeptide	100	*Bacillus subtilis subsp. subtilis* str. 168
3.1	Epipeptide	21,699	Klebsidin (BGC0001639.3)	NRP+Polyketide	40	*Klebsiella pneumoniae*

Region	Type	Cluster size (n.p.)	Most Similar Cluster (MiBIG ID)	Type of product being synthesized	Similarity (%)	The cluster is found in:
3.2	Other	35,411	Bacilysin (BGC0000888.5)	Other	100	*Bacillus sp.* CS93
5.1	NRPS	25,175	Surfactin (xenotetrapeptide BGC0001132.4)	NRP:Lipopeptide	67	*Xenorhabdus nematophila* ATCC 19061
6.1	Sactipeptide, Ranthipeptide	22,954	Sporulation killing factor (BGC0000601.4)	RiPP:Head-to-tailcyclized peptide	100	*Bacillus subtilis subsp. subtilis* str. 168
6.2	NRPS	27,747	Surfactin (bovienimide A BGC0002135.2)	NRP:Lipopeptide	70	*Xenorhabdus bovienii* SS-2004
10.1	NRPS	9,068	Surfactin (bovienimide A BGC0002135.2)	NRP:Lipopeptide	71	*Xenorhabdus bovienii* SS-2004

BGCs exhibiting the maximum degree of similarity to known experimentally characterized clusters were localized in regions 1.2, 1.3, 1.5, 2.1, 2.2, 2.3, 3.2, and 6.1. In contrast, BGCs with undetermined product types, designated as terpenes and epipeptides, were identified in regions 1.1, 1.4, 1.7, and 3.1 (Table 3).

Region 1.2 encompasses genes encoding enzymes such as T3PKS, NRPS, and trans-AT PKS.

The BGC for bacillibactin (BGC0000309, Region 2.1) encodes a catecholate siderophore. Notably, the BAGEL4 and PRISM 4 servers identified the ComX pheromone cluster within this same region (Supplement Table S2).

The group of siderophores also includes pulcherriminic acid (BGC0002103), which is encoded by a BGC in region 2.2.

Bacilysin biosynthetic gene cluster was found in region 3.2. This identified cluster (BGC0000888) displays 100% sequence identity to the corresponding clusters in the genomes of the model biocontrol strain *Bacillus velezensis* FZB42 and *Bacillus* sp. CS93.

In region 4, the BAGEL4 server identified a BGC for sactipeptides (sulfur-to-alpha-carbon thioether cross-linked peptides).

Furthermore, within regions 5.1, 6.2, and 10.1, the *srfAA-AB* gene clusters encoding the lipopeptide surfactin were localized. Initial antiSMASH analysis indicated relatively low similarity scores for these clusters compared to known reference metabolites. To resolve this, the amino acid sequences of the core biosynthetic genes were further scrutinized using BLASTp (https://blast.ncbi.nlm.nih.gov/Blast.cgi). The analysis confirmed high sequence identity with reference proteins from *B. subtilis* subsp. *subtilis* str. 168:

- Surfactin synthase subunit 2 (Q04747.3) – 100% identity;
- Surfactin synthase subunit 1 (P27206.4) – 98.8% identity;

- Surfactin synthase subunit 3 (Q08787.2) – 98.27% identity.

According to the MiBIG database analysis, the products synthesized in certain regions are also associated with various lipotripeptides, specifically xenotetrapeptide (BGC0001132) and bovienimide A (BGC0002135) (Fig. 4). In regions 1.5, 2.3, and 6.1, gene clusters responsible for bacteriocin synthesis were identified (Table 3 and Supplement Table S2).

Supplement Table S2 provides a comparative analysis of the BGC screening results obtained using different bioinformatics platforms. Overall, the identified cluster types and their genomic localizations are highly consistent across the tools, although minor variations were observed.

Specifically, the BAGEL4 server identified a sactipeptide biosynthetic cluster on contig 4. Subsequent BLASTp analysis against the UniProt database identified the core gene of this sequence as the hypothetical protein YfkA (YFKA_BACSU). Furthermore, the PRISM 4 software identified an NRPS cluster of unknown function on contig 2 (nucleotides 101,773–111,515), as detailed in Supplement Table 2.

Metabolomic analysis

UPLC–HRMS analysis of the *B. subtilis* ONU 1125 exometabolome in positive ionization mode enabled the putative annotation of 20 metabolites (Table 4). The identified compounds encompass several chemical classes, including lipopeptides, polyketides, cyclic dipeptides, as well as an NRPS-PKS hybrid and a phenazine-like derivative.

Notably, surfactins were detected in the metabolome of the strain (Table 4, Supplement Fig S1). This identification is in high agreement with the genomic analysis, which localized and annotated the corresponding biosynthetic gene clusters (Table 3 and Supplement Table 2).

Table 4
Putatively annotated metabolites in the exometabolome of *Bacillus subtilis* ONU 1125 detected by UPLC-MS analysis

Class	Compound	Dominant peak, $[M+H]^+$ [m/z]	Adduct [m/z]	RT [min]	Activity / properties
Polyketides	Plakinic acid K/M	419.3168	441.2995 $[M+Na]^+$	19.59	Antifungal [14]
	16-demethylgymnodimine D	510.3200	532.3027 $[M+Na]^+$	12.65	–
Lipopeptides	Gageostatin A	1040.6854	1062.6676 $[M+Na]^+$	15.45	Antifungal (phytopathogens), cytotoxic, antitumor [15]
	Gageostatin B	1054.7012	1076.6857 $[M+Na]^+$	15.91	
	Gageostatin C	1008.6598	1030.6429 $[M+Na]^+$	16.69	
	Bacircin 1	1008.6599	1030.6423 $[M+Na]^+$	17.20	Antibacterial (gram-positive, gram-negative), cytotoxic, antitumor [16]
	Bacircin 2	1022.6757	1044.6564 $[M+Na]^+$	17.80	
	Bacircin 3	1022.6751	1060.6281 $[M+K]^+$	17.32	
	Surfactin B1/B2	1022.6751	1060.6281 $[M+K]^+$	17.32	Antibacterial (gram-positive, gram-negative), antifungal (phytopathogens – *Fusarium oxysporum*, *Rhizoctonia solani*), cytotoxic, antitumor, immunomodulatory [17]
	Surfactin C1	1036.6907	1058.6752 $[M+Na]^+$	18.47	
	4-L- alaninesurfactin B2/B1	994.6437	1016.627 $[M+Na]^+$	16.19	
Cyclic dipeptides	Cyclo(leucine proline)	211.1446	233.1264 $[M+Na]^+$	4.03	Antibacterial (antivirulent, antibiofilm), antifungal – inhibits aflatoxin production

Class	Compound	Dominant peak, $[M + H]^+$ [m/z]	Adduct [m/z]	RT [min]	Activity / properties
					Aspergillus parasiticus [18, 19]
	Cyclo(isoleucine proline)	211.1449	233.1268 $[M + Na]^+$	3.89	Antibacterial (gram-positive), antifungal (*Aspergillus niger*) [20]
	Cyclo(alanyl phenyl alanyl)	219.1135	437.2195 $[2M + H]^+$	3.58	–
	Cyclo(prolyltyrosine) L-L	261.1240	283.1064 $[M + Na]^+$	2.46	Antioxidant, antibacterial (gram-negative *Xanthomonas axopodis, Ralstonia solanacearum* – phytopathogens) [21]
	Cyclo(prolyltyrosine) D-L	261.1241	283.1064 $[M + Na]^+$	2.61	
	Cyclo(prolyltryptophyl)	284.1400	306.122 $[M + Na]^+$	4.82	Antibacterial (gram-positive), antifungal – *Trichophyton rubrum, Cryptococcus neoformans, Candida albicans* [22]
	Cyclo(phenyl alanyl phenyl alanyl)	295.1447	336.1701 $[M + ACN+H]^+$	6.53	Quorum sensing inhibitor, cytotoxic, antitumor [23]
NRPS-PKS hybrids	Tamandarin A-like compound	1056.6233	1078.6027 $[M + Na]^+$	14.93	Antitumor, cytotoxicity [24]
Phenazine derivatives	Phenazine-like derivative	211.0871	421.1663 $[2M + H]^+$	7.90	Cytotoxic activity against murine leukemia P388 cells; deep-sea *Bacillus*-derived phenazine derivative [25]

The *B. subtilis* ONU 1125 strain was found to synthesize two primary surfactin variants, categorized as surfactin B and surfactin C, based on specific substitutions within their peptide moieties. Surfactin B incorporates L-valine, whereas surfactin C harbors L-isoleucine at the amino acid position involved in the formation of the macrocyclic lactone ring with C14–C15 *β*-hydroxy fatty acids. Mass spectrometric analysis in positive ionization mode revealed characteristic clusters of ions. Specifically, signals at m/z 1022.6751 $[M + H]^+$ and 1060.6281 $[M + K]$+ were identified as surfactin B1/B2 adducts. Furthermore, ions at m/z 1036.6907 $[M + H]^+$ and 1058.6752 $[M + Na]^+$ confirmed the presence of surfactin C1 (Supplement Fig S1).

Beyond the canonical surfactins B and C, UPLC-MS analysis of the *B. subtilis* ONU 1125 metabolomic profile revealed the presence of [4-L-alanine]-surfactin B2/B1 with m/z 994.6437 $[M + H]^+$ and 1016.6270 $[M + Na]^+$ (Table 4, Supplement Fig S1). This variant represents a peptide sequence modification where the L-valine residue at position 4 is substituted by L-alanine, further expanding the structural diversity of the lipopeptides produced by this strain.

The exometabolomic profile of *B. subtilis* ONU 1125 also contained bacircines 1, 2, and 3-surfactin-like cyclic acyl depsipeptides.

The presence of gageostatins A, B, and C was confirmed by the presence of ions at m/z 1040.6854 $[M + H]^+$, 1054.7012 $[M + H]^+$, and 1008.6598 $[M + H]^+$, respectively (Table 4, Supplement Fig S1).

The metabolome of *B. subtilis* ONU 1125 further contained several compounds belonging to the polyketide class, specifically 16-desmethylgymnodimine D, and plakinic acids K/M.

In addition to lipopeptides and polyketides, the metabolic profile featured a diverse array of cyclic dipeptides (diketopiperazines). Among these, the stereoisomers cyclo(L-prolyltyrosyl) and cyclo(D-prolyltyrosyl) were identified together with cyclo(leucylprolyl), cyclo(isoleucylprolyl), cyclo(prolyltryptophyl), and cyclo(phenylalanylphenylalanyl) (Table 4, Supplement Fig S1).

Among the putatively annotated exometabolites of *B. subtilis* ONU 1125, a feature with *m/z* 1056.6233 $[M + H]^+$ and a corresponding sodium adduct at *m/z* 1078.6027 $[M + Na]^+$ was assigned as a tamandarin A-like compound (Table 4).

A feature at *m/z* 211.0871, accompanied by an ion at *m/z* 421.1663 assigned as $[2M + H]^+$, was putatively annotated as a phenazine-like derivative (Table 4).

DISCUSSION

Previous investigations demonstrated that *B. subtilis* ONU 1125 possesses pronounced antagonistic activity against a range of phytopathogenic microorganisms, such as *Pectobacterium carotovorum, Ralstonia solanacearum, Xanthomonas arboricola, Alternaria alternata, Aspergillus flavus, A. niger, A. terreus, Cladosporium cladosporoides, Paecilomyces variotii, Penicillium expansum* with particularly strong activity against *F. oxysporum* [10]. The strain also showed plant growth-promoting activity, positively affecting the growth of barley seedlings [12]. These earlier phenotypic observations provide an important context for the present study: the genomic and exometabolomic data provide a molecular framework for antimicrobial properties that had already been demonstrated experimentally.

Phylogenomic analysis placed *B. subtilis* ONU 1125 in close proximity to the *B. subtilis* type strain ATCC 6051^T, further supporting its taxonomic assignment to this species. Such a phylogenetic relationship provides a taxonomic framework for interpretation of the genomic characteristics of the strain.

The 16 predicted biosynthetic regions indicate a broad capacity for specialized-metabolite production in ONU 1125. Of particular relevance to the previously observed antagonism are BGCs associated with fengycin, surfactin, bacilysin, subtilosin, bacillibactin, and other peptide- or polyketide-related products. Fengycin and

surfactin are well-established contributors to the suppression of phytopathogenic fungi. Fengycin/plipastatin-family compounds can induce hyphal deformation, membrane and cell-wall damage, and conidial lysis, and their production can increase during interactions with phytopathogens such as *F. oxysporum* [26, 27].

The bacilysin BGC and siderophore-associated regions also provide mechanisms relevant to biocontrol. Bacilysin is a broad-spectrum dipeptide antibiotic active against diverse microorganisms, including plant pathogens [28, 29]. Notably, the bacilysin-associated cluster identified in ONU 1125 showed 100% sequence identity to corresponding clusters reported for *B. velezensis* FZB42 and *Bacillus* sp. CS93, strains associated with bacilysin production [30, 31]. This observation further supports the potential functionality of the bacilysin biosynthetic system in ONU 1125.

Bacillibactin and pulcherriminic acid are associated with iron acquisition or extracellular iron sequestration, processes that can influence competition among microorganisms and plant-microbe interactions [32, 33]. The ComX pheromone cluster, located within the same region as the bacillibactin genes, is responsible for the synthesis of a signaling peptide primarily involved in the regulation of genetic competence and biosurfactant production in *B. subtilis*. This peptide is a key component of the quorum-sensing (QS) signaling network and coordinates population-level responses [34].

The biosynthetic architecture of region 1.2, which contains T3PKS-, NRPS-, and trans-AT PKS-associated genes, indicates a substantial capacity for the production of structurally complex secondary metabolites. This region was associated with bacillaene biosynthesis, a polyketide-type natural product previously described in *Bacillus* spp. and linked to antimicrobial activity [35]. The presence of a bacillaene-associated BGC therefore further supports the antimicrobial potential of *B. subtilis* ONU 1125 and may contribute, together with other identified biosynthetic systems, to the antagonistic phenotype previously observed against phytopathogenic microorganisms.

The clearest correspondence between the genomic and metabolomic datasets was observed for the surfactin family. Multiple surfactin-associated NRPS regions were detected in the genome, while the exometabolome contained features putatively annotated as surfactin B1/B2, surfactin C1, and 4-L-alanine-surfactin B2/B1. This concordance strengthens the conclusion that surfactin-family metabolites form part of the bioactive compound profile of ONU 1125. Surfactins are membrane-active biosurfactants with documented antibacterial and antifungal effects and can act synergistically with other *Bacillus* lipopeptides [36, 37]. Such combined activity could contribute to the broad antagonistic phenotype observed for ONU 1125 in previous assays.

Sactipeptide-associated BGCs further expand the predicted antimicrobial potential of *B. subtilis* ONU 1125. These RiPPs contain unusual thioether cross-links and are often involved in antimicrobial activity and microbial competition [38].

The exometabolome also contained features putatively annotated as bacircins, gageostatins, cyclic dipeptides, polyketide-related compounds, a tamandarin A-like compound, and a phenazine-like derivative. Several compounds related to these annotations have reported antimicrobial or antifungal activities. Gageostatins A and B have been documented to inhibit phytopathogenic fungi including *Rhizoctonia solani*, *Colletotrichum acutatum*, and *Botrytis cinerea* [15, 28], whereas several diketopiperazines have been reported to exhibit antibacterial, antifungal, antibiofilm, or quorum-sensing-modulatory activities [18, 19, 20, 21, 22].

The putative annotation of plakinic acid K/M is also noteworthy, as members of the plakinic acid family have demonstrated antifungal activity [14].

The annotation of a putative phenazine-like derivative in the exometabolome of *B. subtilis* ONU 1125 is noteworthy, as only a few reports have described phenazine-related compounds in *Bacillus*, including N-glucosylated derivatives formed through biotransformation of *Pseudomonas*-derived phenazine-1-carboxylic acid by *Bacillus* sp. [39], and a cytotoxic phenazine derivative isolated from a deep-sea *Bacillus* sp. from Pacific Ocean [25]. A parallel can be drawn with the mentioned work of Li et al. [25], who isolated a novel cytotoxic phenazine derivative with a unique ring structure from a deep-sea *Bacillus* sp. recovered from Pacific Ocean sediments at a depth of 5,059 m - an ecological context similar to that of *B. subtilis* ONU 1125, isolated from Black Sea bottom sediments at 1,537 m. In both cases, the strains originated from deep-sea benthic environments, raising the possibility that the capacity to produce phenazine-related compounds may be associated with deep-sediment *Bacillus* ecotypes. However, this hypothesis requires further investigation using additional deep-sea isolates and targeted metabolomic analyses.

Further investigation is also required for the putatively annotated tamandarin A-like compound, a cyclic depsipeptide structurally related to the didemnin family [40, 41, 42]. Closely related didemnins are produced by marine bacteria of the genus *Tistrella* through a large hybrid NRPS–PKS biosynthetic gene cluster [40, 41], and heterologous production from the didemnin BGC has also been demonstrated in *Streptomyces* [42]. Thus, the tamandarin A-like feature detected in ONU 1125 may represent a structurally related NRPS–PKS-derived depsipeptide.

Studies combining activity-guided fractionation and expression analysis under pathogen-interaction conditions will be important for further characterizing the compounds responsible for the antimicrobial phenotype of *B. subtilis* ONU 1125.

CONCLUSIONS

Integrated genomic and exometabolomic analyses revealed a broad biosynthetic potential in the Black sea deep-sediment strain *Bacillus subtilis* ONU 1125. Together with the previously demonstrated antagonistic activity of ONU 1125 against phytopathogenic microorganisms, these findings provide a molecular framework for the biological properties of the strain. *B. subtilis* ONU 1125 represents a promising candidate for further investigation as a source of antimicrobial metabolites and as a potential biological control agent.

MATERIALS AND METHODS

Bacterial strain and cultivation conditions

The study focused on the strain *Bacillus subtilis* ONU 1125 isolated from deep-sea bottom sediment samples of the Black Sea (N 41° 32.670', E 37° 37.460'). The samples were collected at a depth of 1,537 m from a core horizon of 5–10 cm during the M84/2 expedition of the University of Bremen aboard the research vessel Meteor in March 2011 and kindly provided by the Institute of Marine Biology of the National Academy of Sciences of Ukraine.

The strain was initially identified based on its core biological properties and fatty acid methyl ester (FAME) profile [43]. The strain is maintained in the Collection of Marine and Biotechnologically Useful Microorganisms at Odesa I.I. Mechnikov National University, cryopreserved in nutrient broth supplemented with 30% (v/v) glycerol at -84°C.

Genomic DNA extraction and sequencing

Genomic DNA was extracted from overnight cultures of *B. subtilis* ONU 1125 grown in nutrient broth using a modified isolation method [44]. To ensure high purity, the resuspended DNA samples were treated with 20 µl of pre-activated RNase (5 µg/ml) and incubated at 37°C for 3–4 hours with gentle periodic mixing. The quality and concentration of the extracted DNA were assessed using a DeNovix DS-11FX+ spectrophotometer and verified via horizontal electrophoresis on a 1.5% agarose gel at 150 V for 40 minutes.

Whole-genome sequencing (WGS) was performed using a hybrid approach combining Illumina HiSeq 4000 (2x150 bp) and Oxford Nanopore MinION (Flongle FLG-001) platforms at Explogen LLC (Lviv, Ukraine).

The Whole Genome Shotgun project for *Bacillus subtilis* ONU 1125 has been deposited at DDBJ/ENA/GenBank under the accession number JBZVEQ000000000.

2.3. Genome annotation and visualization

Genome annotation was performed using the Pathosystems Resource Integration Center (PATRIC) server, a component of the Bacterial and Viral Bioinformatics Resource Center (BV-BRC) web resource (www.bv-brc.org) [45]. A circular representation of the genome assembly was generated using the CGView Server through the Proksee platform (https://proksee.ca/) [46].

Taxonomic identification and phylogenetic analysis

To confirm the species identity of the investigated strain as *B. subtilis*, genomic data were analyzed using the KmerFinder-3.2 tool, hosted by the Center for Genomic Epidemiology (https://www.genomicepidemiology.org/) [47]. For precise taxonomic placement and high-resolution classification, a comprehensive phylogenetic assessment was conducted using the Type Strain Genome Server (TYGS) (https://tygs.dsmz.de/) enabling the calculation of digital DNA–DNA hybridization (dDDH) values via the Genome-to-Genome Distance Calculator (GGDC) [48, 49]. The resulting phylogeny was reconstructed based on average branch support values and δ statistics to ensure the robustness and accuracy of the taxonomic assignment [50]. The phylogenetic tree was subsequently visualized and graphically refined using Interactive Tree Of Life (iTOL) v6, with adjustments limited to line type and font size [51].

Identification of biosynthetic gene clusters (BGCs) associated with secondary metabolites

To identify BGCs, a multi-tool bioinformatics pipeline was employed, including antiSMASH version 8.0.4 (https://antismash.secondarymetabolites.org) [52], BAGEL4 (http://bagel.molgenrug.nl) [53, 54], PRISM 4

(https://prism.kapoosecreek.com) [55], and GECCO (https://github.com/zellerlab/GECCO) [56]. The utilization of an expanded suite of tools was justified by the distinct underlying algorithms designed for BGC detection.

Specifically, antiSMASH was used to identify type I and type II polyketide synthases (PKSs) and non-ribosomal peptide synthetases (NRPSs). BAGEL4 focused on the detection of ribosomally synthesized and post-translationally modified peptides (RiPPs). PRISM 4 was applied to predict the chemical structures of bacterial antibiotics, while GECCO was employed to identify novel or cryptic BGCs. The predicted products of the identified NRPS clusters were further cross-referenced and validated using the NORINE database (https://norine.univ-lille.fr/norine/) [57].

Individual antiSMASH images were combined into a composite figure using custom Python scripts for panel arrangement and font formatting; no other elements or scientific content were modified. The scripts are available on GitHub: https://github.com/Typhoidfever/bacillus_subtilis_onu_1125

Extraction of secondary metabolites

B. subtilis ONU 1125 was cultivated for 4 days in Gause No. 1 liquid medium supplemented with 0.5% tryptone. Cultivation was performed using a rotary shaker at 220 rpm and a constant temperature of 28°C. Following incubation, the culture broth was centrifuged at 10,000 × g for 10 minutes at 18°C to separate the biomass from the cell-free supernatant.

Secondary exometabolites were extracted from the supernatant using ethyl acetate in a 1:1 (v/v) ratio. The mixture was subjected to gentle agitation on a horizontal shaker for 2 hours at room temperature. After clear phase separation, the organic layer containing the metabolites was carefully collected. The ethyl acetate was subsequently evaporated at 40°C under a steady stream of nitrogen gas (pressure ≤ 2 psi) using a Techne Sample Concentrator FSC 400D equipped with a DB 100/3 Dri-Block Heater [58].

Analysis of exometabolite spectra

The extracted metabolites were dissolved in dimethyl sulfoxide (DMSO). Sample analysis was performed using a Thermo Fisher Dionex UltiMate 3000 BioRS UPLC system coupled with a Bruker Daltonics maXis II mass spectrometer (4G hr-ToF). Chromatographic separation was achieved on a Waters BEH C18 column (100 mm × 2.1 mm, 1.7 µm) maintained at a column oven temperature of 45°C and a flow rate of 0.5 mL/min.

The mobile phase consisted of (A) 0.1% formic acid in water and (B) 100% acetonitrile containing 0.1% formic acid. The separation was performed using the following gradient program: 0–1 min, 5% B; 1–19 min, a linear gradient from 5% to 95% B; followed by an isocratic hold at 95% B for 1 min.

Mass spectra were acquired in the positive ionization mode within an *m/z* range of 150–2000. To confirm the assignment of peaks as $[M + H]^+$ ions, the spectra were screened for the presence of characteristic adducts. Identified compounds were cross-referenced against the Dictionary of Natural Products database using a mass tolerance of ± 3 ppm relative to the calculated exact molecular mass (*X*).

Declarations

Acknowledments

The authors gratefully acknowledge the late Dr. Yu. P. Zaitsev and the late Dr. B. G. Aleksandrov (Institute of Marine Biology of the National Academy of Sciences of Ukraine) for kindly providing the deep-sea sediment samples used in this study.

Data Availability

The genome sequence data generated in this study are available in DDBJ/ENA/GenBank under the Whole Genome Shotgun accession JBZVEQ000000000.

Conflicts of interest

The authors declare that they have no known competing financial interests or personal relationships that could have appeared to influence the work reported in this paper.

Funding

This work was supported by the Ministry of Education and Science of Ukraine (2024–2026, project No. 0124U001029 “Development of a biotechnology for the ecologization of cereal crop production using marine biological resources to restore the fertility of soils affected by military actions”).

Author Contributions

Conception and design: M.P., N.V., V.I. Functional studies: N.V., M.S., O.A., I.S., V.S., H.L., A.O., T.I. Data analysis and interpretation: N.V., M.G., M.S., A.O., V.I., R.W. Drafting the manuscript: all authors. Critical revision of the manuscript: all authors. Supervision: V.I., M.P., M.G., R.W.

References

1. Harirchi, S. et al. Bacillales: from taxonomy to biotechnological and industrial perspectives. *Microorganisms* **10**, 2355. https://doi.org/10.3390/microorganisms10122355 (2022).
2. Patyka, M., Wang, R., Honchar, A., Patyka, T. & Khablak, S. Modulation of the rhizosphere microbiome structure and optimization of beneficial functions in winter wheat induced by *Bacillus subtilis*: a metagenomic and phenotypic study. *FEMS Microbiol. Ecol.* **101**, fiaf097. https://doi.org/10.1093/femsec/fiaf097 (2025).
3. Xiao, S. et al. Secondary metabolites from marine-derived *Bacillus*: a comprehensive review of origins, structures, and bioactivities. *Mar. Drugs*. **20**, 567. https://doi.org/10.3390/md20090567 (2022).
4. Ostapchuk, A. M., Shtenikov, M. D. & Ivanytsia, V. O. Exometabolites of endospore-forming bacteria of *Bacillus* genus identified by genomic-metabolomic profiling. *Ukr. Biochem. J.* **92**, 154–164. https://doi.org/10.15407/ubj92.06.154 (2020).
5. Shehata, A. S. et al. Isolation and identification of antifungal, antibacterial and nematocide agents from marine *Bacillus gottheilii* MSB1. *BMC Biotechnol.* **24**, 92. https://doi.org/10.1186/s12896-024-00920-y (2024).

6. Rathod, K., Rana, S., Dhandukia, P. & Thakker, J. N. Investigating marine *Bacillus* as an effective growth promoter for chickpea. *J. Genet. Eng. Biotechnol.* **21**, 137. https://doi.org/10.1186/s43141-023-00608-4 (2023).
7. Khatri, S., Dubey, S., Shivay, Y. S., Jelsbak, L. & Sharma, S. Organic farming induces changes in bacterial community and disease suppressiveness against fungal phytopathogens. *Appl. Soil. Ecol.* **181**, 104658. https://doi.org/10.1016/j.apsoil.2022.104658 (2023).
8. Kiesewalter, H. T. et al. Genomic and chemical diversity of *Bacillus subtilis* secondary metabolites against plant pathogenic fungi. *mSystems* 6, e00770-20 (2021). https://doi.org/10.1128/mSystems.00770-20
9. Chen, J. et al. Genomic and metabolomic insights into the antimicrobial compounds and plant growth-promoting potential of *Bacillus velezensis* B115. *Sci. Rep.* **15**, 10666. https://doi.org/10.1038/s41598-025-92322-z (2025).
10. Andriushchenko, O. V. et al. Evaluation of antagonistic activity of Bacilli against phytopathogenic microorganisms. *Microbiol. Biotechnol.* **1**, 6–24. https://doi.org/10.18524/2307-4663.2025.1(63).327097 (2025).
11. Strashnova, I. V. & Andriuschenko, O. V. Antimicrobial activity of soil Bacilli against phytopathogenic microorganisms isolated from affected cereal plants. *Microbiol. Biotechnol.* **2**, 6–16. https://doi.org/10.18524/2307-4663.2023.2(58).286959 (2023).
12. Andriushchenko, O. V., Strashnova, I. V., Ivanytsia, T. V., Ivanytsia, V. O. & Galkin, M. B. Assessment of strain-dependent variation of phytostimulatory activity in *Streptomyces ambofaciens*-based bioformulations for agricultural applications. *Regul. Mech. Biosyst*. **16**, e25206. https://doi.org/10.15421/0225206 (2025).
13. Ivanytsia, V. O., Shtenikov, M. D. & Ostapchuk, A. M. Facultatively-anaerobic endospore forming bacteria of deep water bottom sediments of Black Sea. *Microbiol. Biotechnol.* **4**, 94–103. https://doi.org/10.18524/2307-4663.2017.4(40).119560 (2017).
14. Jamison, M. T., Dalisay, D. S. & Molinski, T. F. Peroxide natural products from *Plakortis zyggompha* and the sponge association *Plakortis halichondrioides–Xestospongia deweerdtae*: antifungal activity against *Cryptococcus gattii*. *J. Nat. Prod.* **79**, 555–563. https://doi.org/10.1021/acs.jnatprod.5b00951 (2016).
15. Tareq, F. S. et al. Gageostatins A–C, antimicrobial linear lipopeptides from a marine *Bacillus subtilis*. *Mar. Drugs*. **12**, 871–885. https://doi.org/10.3390/md12020871 (2014).
16. Das, P., Mukherjee, S., Sivapathasekaran, C. & Sen, R. Microbial surfactants of marine origin: potentials and prospects. In Biosurfactants (ed Sen, R.) Vol. 672 (Springer, https://doi.org/10.1007/978-1-4419-5979-9_7 (2010).
17. Ding, W. et al. Structures and antitumor activities of ten new and twenty known surfactins from the deep-sea bacterium *Limimaricola* sp. SCSIO 53532. *Bioorg. Chem.* **120**, 105589. https://doi.org/10.1016/j.bioorg.2021.105589 (2022).
18. Gowrishankar, S. et al. Cyclic dipeptide cyclo(L-leucyl-L-prolyl) from marine *Bacillus amyloliquefaciens* mitigates biofilm formation and virulence in *Listeria monocytogenes*. *Pathog. Dis.* 74, ftw017 (2016). https://doi.org/10.1093/femspd/ftw017
19. Yan, P. S. et al. Cyclo(L-leucyl-L-prolyl) produced by *Achromobacter xylosoxidans* inhibits aflatoxin production by *Aspergillus parasiticus*. *Appl. Environ. Microbiol.* **70**, 7466–7473.

https://doi.org/10.1128/AEM.70.12.7466-7473.2004 (2004).

20. Song, Z., Hou, Y., Yang, Q., Li, X. & Wu, S. Structures and biological activities of diketopiperazines from marine organisms: a review. *Mar. Drugs*. **19**, 403. https://doi.org/10.3390/md19080403 (2021).
21. Wattana-Amorn, P., Charoenwongsa, W., Williams, C., Crump, M. P. & Apichaisataienchote, B. Antibacterial activity of cyclo(L-Pro-L-Tyr) and cyclo(D-Pro-L-Tyr) from *Streptomyces* sp. strain 22 – 4 against phytopathogenic bacteria. *Nat. Prod. Res.* **30**, 1980–1983. https://doi.org/10.1080/14786419.2015.1095747 (2016).
22. Kumar, S. N., Nath, V. S., Chandran, R. P. & Nambisan, B. Cyclic dipeptides from rhabditid entomopathogenic nematode-associated *Bacillus cereus* have antimicrobial activities. *World J. Microbiol. Biotechnol.* **30**, 439–449. https://doi.org/10.1007/s11274-013-1461-7 (2014).
23. Chen, J. et al. Quorum sensing inhibitors from marine microorganisms and their synthetic derivatives. *Mar. Drugs*. **17**, 80. https://doi.org/10.3390/md17020080 (2019).
24. Vervoort, H., Fenical, W., Epifanio, R. A. & Tamandarins A and B: new cytotoxic depsipeptides from a Brazilian ascidian of the family Didemnidae. *J. Org. Chem.* **65**, 782–792. https://doi.org/10.1021/jo991425a (2000).
25. Li, D. et al. A new cytotoxic phenazine derivative from a deep sea bacterium *Bacillus* sp. *Arch. Pharm. Res.* **30**, 552–555. https://doi.org/10.1007/BF02977647 (2007).
26. Zhang, X. et al. Lipopeptides, a novel protein, and volatile compounds contribute to the antifungal activity of the biocontrol agent *Bacillus atrophaeus* CAB-1. *Appl. Environ. Microbiol.* **97**, 9525–9534. https://doi.org/10.1007/s00253-013-5198-x (2013).
27. Zhang, L., Sun, C. & Fengycins cyclic lipopeptides from marine *Bacillus subtilis* strains, kill the plant-pathogenic fungus *Magnaporthe grisea* by inducing reactive oxygen species production and chromatin condensation. *Appl. Environ. Microbiol.* **84**, e00445–e00418. https://doi.org/10.1128/AEM.00445-18 (2018).
28. Kaspar, F., Neubauer, P. & Gimpel, M. Bioactive secondary metabolites from *Bacillus subtilis*: a comprehensive review. *J. Nat. Prod.* **82**, 2038–2053. https://doi.org/10.1021/acs.jnatprod.9b00110 (2019).
29. Islam, T., Rabbee, M. F., Choi, J. & Baek, K. H. Biosynthesis, molecular regulation, and application of bacilysin produced by *Bacillus* species. *Metabolites* **12**, 397. https://doi.org/10.3390/metabo12050397 (2022).
30. Chen, X. H. et al. Difficidin and bacilysin produced by plant-associated *Bacillus amyloliquefaciens* are efficient in controlling fire blight disease. *J. Biotechnol.* **140**, 38–44. https://doi.org/10.1016/j.jbiotec.2008.10.015 (2009).
31. Phister, T. G., O'Sullivan, D. J. & McKay, L. L. Identification of bacilysin, chlorotetaine, and iturin A produced by *Bacillus* sp. strain CS93 isolated from pozol, a Mexican fermented maize dough. *Appl. Environ. Microbiol.* **70**, 631–634. https://doi.org/10.1128/AEM.70.1.631-634.2004 (2004).
32. Chakraborty, K., Kizhakkepatt-Kizhakkekalam, V., Joy, M. & Chakraborty, R. D. Bacillibactin class of siderophore antibiotics from a marine symbiotic *Bacillus* as promising antibacterial agents. *Appl. Microbiol. Biotechnol.* **106**, 329–340. https://doi.org/10.1007/s00253-021-11632-0 (2022).

33. Angelini, L. L. et al. Pulcherrimin protects *Bacillus subtilis* against oxidative stress during biofilm development. *npj Biofilms Microbiomes*. **9**, 50. https://doi.org/10.1038/s41522-023-00418-z (2023).
34. Treinen, C. et al. Modeling the time course of ComX: towards molecular process control for *Bacillus* wild-type cultivations. *AMB Express*. **11**, 144. https://doi.org/10.1186/s13568-021-01306-5 (2021).
35. Miao, S., Liang, J., Xu, Y., Yu, G. & Shao, M. Bacillaene, sharp objects consist in the arsenal of antibiotics produced by *Bacillus*. *J. Cell. Physiol.* **239**, e30974. https://doi.org/10.1002/jcp.30974 (2024).
36. Chen, X. et al. A mini-review: mechanism of antimicrobial action and application of surfactin. *World J. Microbiol. Biotechnol.* **38**, 143. https://doi.org/10.1007/s11274-022-03323-3 (2022).
37. Rafiee, F., Fazeli, M. R., Sepahi, A. A. & Noormohammadi, Z. Isolation, screening and identification of native and new *Bacillus subtilis* with strong antifungal compound against *Fusarium oxysporum*. *Biocontrol Sci.* **27**, 201–208. https://doi.org/10.4265/bio.27.201 (2022).
38. Tran, C., Cock, I. E., Chen, X. & Feng, Y. Antimicrobial *Bacillus*: metabolites and their mode of action. *Antibiotics* **11**, 88. https://doi.org/10.3390/antibiotics11010088 (2022).
39. Iloabuchi, K. & Spiteller, D. *Bacillus* sp. G2112 detoxifies phenazine-1-carboxylic acid by N5 glucosylation. *Molecules* 29, 589 (2024). https://doi.org/10.3390/molecules29030589
40. Xu, Y. et al. Bacterial biosynthesis and maturation of the didemnin anti-cancer agents. *J. Am. Chem. Soc.* **134**, 8625–8632. https://doi.org/10.1021/ja301735a (2012).
41. Stankey, R. J., Johnson, D., Duggan, B. M. & Mead, D. A. La Clair, J. J. A survey of didemnin depsipeptide production in *Tistrella*. *Mar. Drugs*. **21**, 56. https://doi.org/10.3390/md21020056 (2023).
42. Zhang, H. et al. Exploring the biosynthetic potential of *Tistrella* species for producing didemnin antitumor agents. *ACS Chem. Biol.* **19**, 2176–2185. https://doi.org/10.1021/acschembio.4c00384 (2024).
43. Ivanytsia, V. O., Shtenikov, M. D. & Ostapchuk, A. M. Facultatively-anaerobic endosporeforming bacteria of deep water bottom sediments of Black Sea. *Microbiol. Biotechnol.* **4**, 94–103. https://doi.org/10.18524/2307-4663.2017.4(40).119560 (2017).
44. De, S. et al. A simple method for the efficient isolation of genomic DNA from Lactobacilli isolated from traditional Indian fermented milk (dahi). *Indian J. Microbiol.* **50**, 412–418. https://doi.org/10.1007/s12088-011-0079-4 (2010).
45. Wattam, A. R. et al. Assembly, annotation, and comparative genomics in PATRIC, the all bacterial bioinformatics resource center. *Methods Mol. Biol.* **1704**, 79–101. https://doi.org/10.1007/978-1-4939-7463-4_4 (2018).
46. Grant, J. R. et al. Proksee: in-depth characterization and visualization of bacterial genomes. *Nucleic Acids Res.* **51**, W484–W492. https://doi.org/10.1093/nar/gkad326 (2023).
47. Hasman, H. et al. Rapid whole-genome sequencing for detection and characterization of microorganisms directly from clinical samples. *J. Clin. Microbiol.* **52**, 139–146. https://doi.org/10.1128/JCM.02452-13 (2014).
48. Meier-Kolthoff, J. P. & Göker, M. TYGS is an automated high-throughput platform for state-of-the-art genome-based taxonomy. *Nat. Commun.* **10**, 2182. https://doi.org/10.1038/s41467-019-10210-3 (2019).
49. Meier-Kolthoff, J. P., Sardà Carbasse, J., Peinado-Olarte, R. L. & Göker, M. TYGS and LPSN: a database tandem for fast and reliable genome-based classification and nomenclature of prokaryotes. *Nucleic Acids Res.* **50**, D801–D807. https://doi.org/10.1093/nar/gkab902 (2022).

50. Holland, B. R., Huber, K. T., Dress, A. & Moulton, V. δ plots: a tool for analyzing phylogenetic distance data. *Mol. Biol. Evol.* **19**, 2051–2059. https://doi.org/10.1093/oxfordjournals.molbev.a004030 (2002).
51. Letunic, I. & Bork, P. Interactive Tree of Life (iTOL) v6: recent updates to the phylogenetic tree display and annotation tool. *Nucleic Acids Res.* **52**, W78–W82. https://doi.org/10.1093/nar/gkae268 (2024).
52. Blin, K. et al. antiSMASH 8.0: extended gene cluster detection capabilities and analyses of chemistry, enzymology, and regulation. *Nucleic Acids Res.* **53**, W32–W38. https://doi.org/10.1093/nar/gkaf334 (2025).
53. van Heel, A. J. et al. BAGEL4: a user-friendly web server to thoroughly mine RiPPs and bacteriocins. *Nucleic Acids Res.* **46**, W278–W281. https://doi.org/10.1093/nar/gky383 (2018).
54. Agrawal, P., Amir, S., Deepak, Barua, D. & Mohanty, D. RiPPMiner-Genome: a web resource for automated prediction of crosslinked chemical structures of RiPPs by genome mining. *J. Mol. Biol.* **433**, 166887. https://doi.org/10.1016/j.jmb.2021.166887 (2021).
55. Skinnider, M. A. et al. Comprehensive prediction of secondary metabolite structure and biological activity from microbial genome sequences. *Nat. Commun.* **11**, 6058. https://doi.org/10.1038/s41467-020-19986-1 (2020).
56. Carroll, L. M. et al. Accurate de novo identification of biosynthetic gene clusters with GECCO. *bioRxiv* Preprint at (2021). https://doi.org/10.1101/2021.05.03.442509
57. Flissi, A. et al. Norine: update of the nonribosomal peptide resource. *Nucleic Acids Res.* **48**, D465–D469. https://doi.org/10.1093/nar/gkz1000 (2020).
58. Paulus, C. et al. New natural products identified by combined genomics-metabolomics profiling of marine *Streptomyces* sp. MP131-18. *Sci. Rep.* **7**, 42382. https://doi.org/10.1038/srep42382 (2017).
59. Acknowledments.
60. The authors gratefully acknowledge the late Dr. Yu. P. Zaitsev and the late Dr. B. G. Aleksandrov (Institute of Marine Biology of the National Academy of Sciences of Ukraine) for kindly providing the deep-sea sediment samples used in this study.

Figures

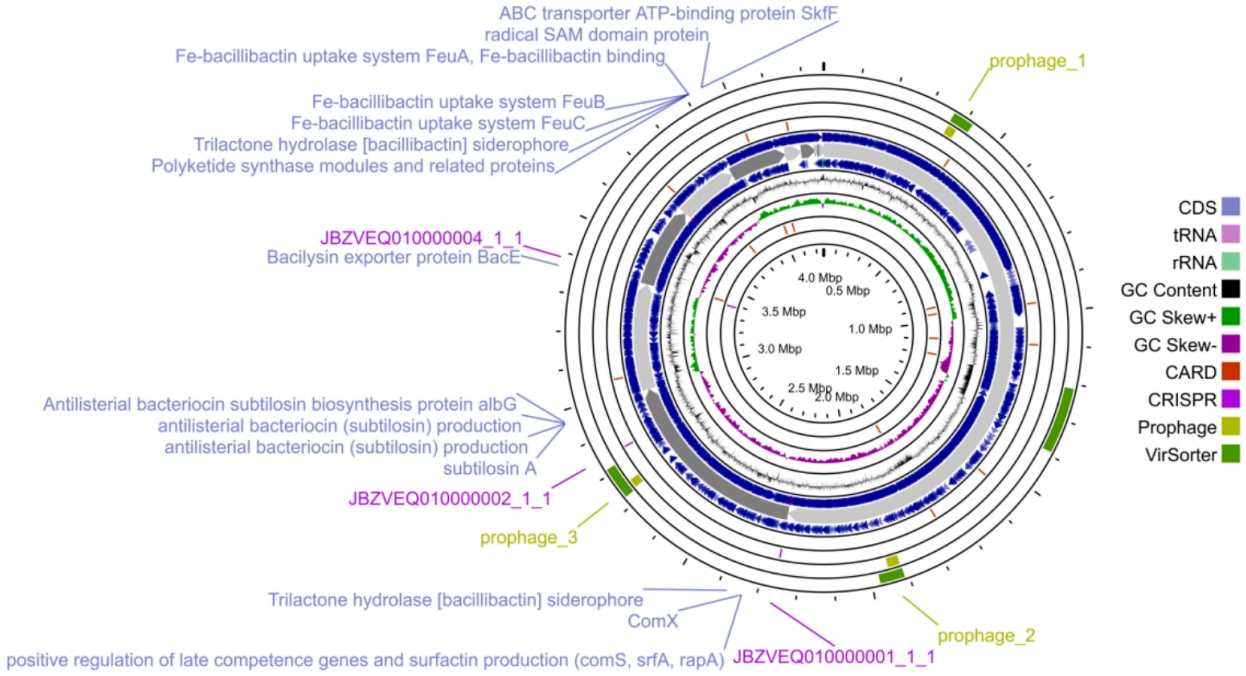


Figure 1

Genome architecture of *Bacillus subtilis*ONU 1125. Circular representation of the 11-contig genome assembly highlighting key functional regions, including CRISPR loci, antibiotic resistance determinants, and identified prophage regions.

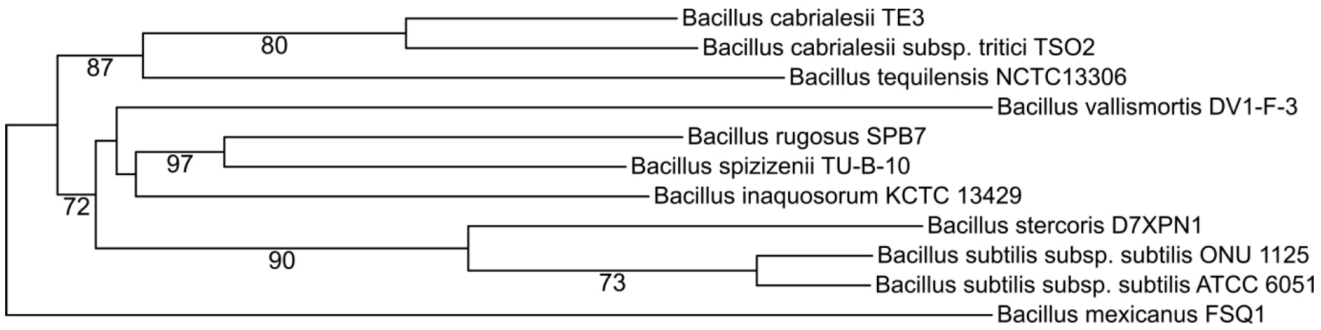


Figure 2

Whole-genome phylogeny of Bacillus subtilis ONU 1125. Phylogenetic tree of *B. subtilis* ONU 1125reconstructed and visualized based on whole-genome sequencing data and digital DNA–DNA hybridization (dDDH)analysis.

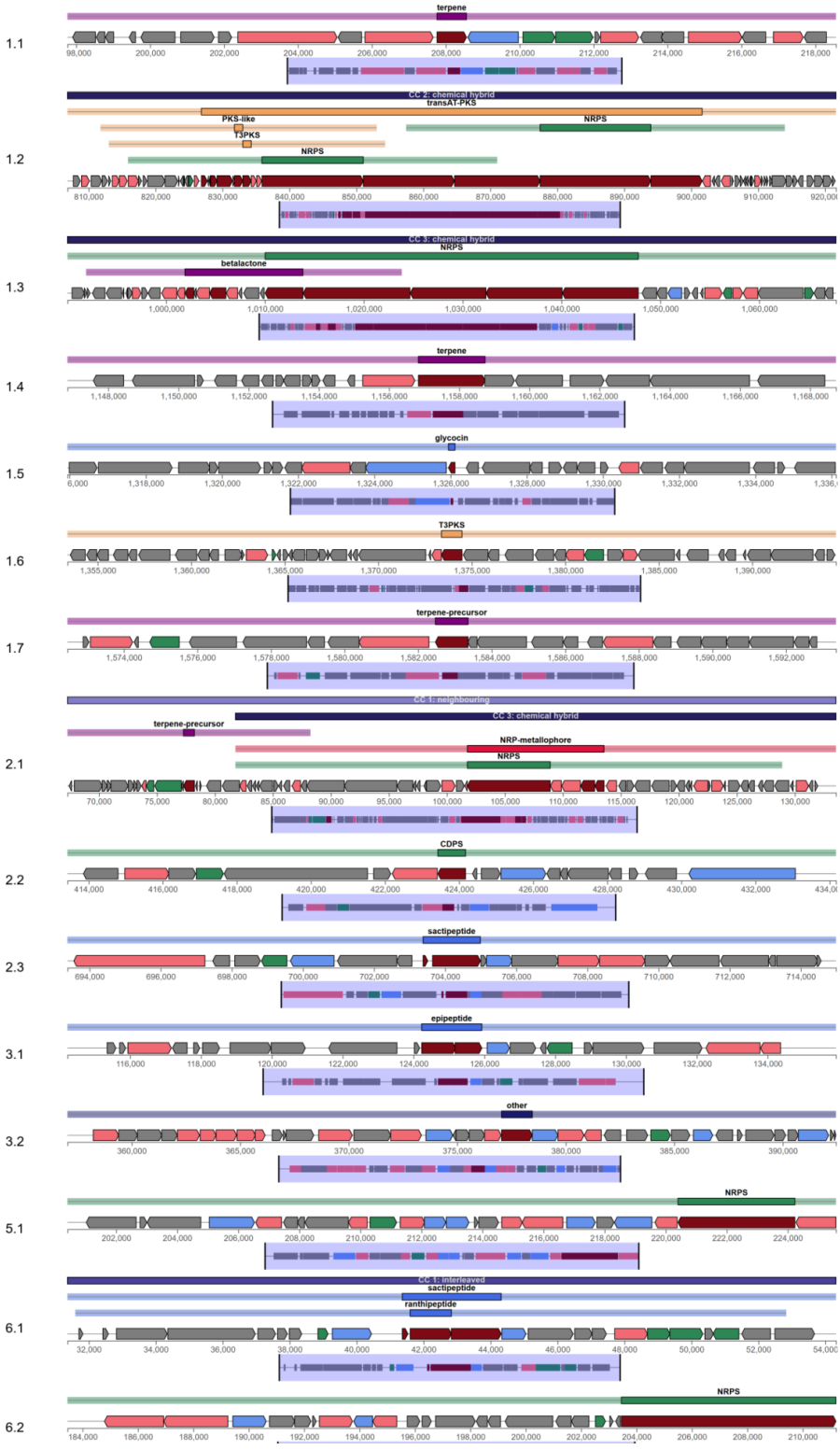


Figure 3

Biosynthetic gene clusters identified in the genome of *Bacillus subtilis* ONU 1125. Representation of BGCs for secondary metabolites identified in the *Bacillus subtilis* ONU 1125 genome using the antiSMASH pipeline.

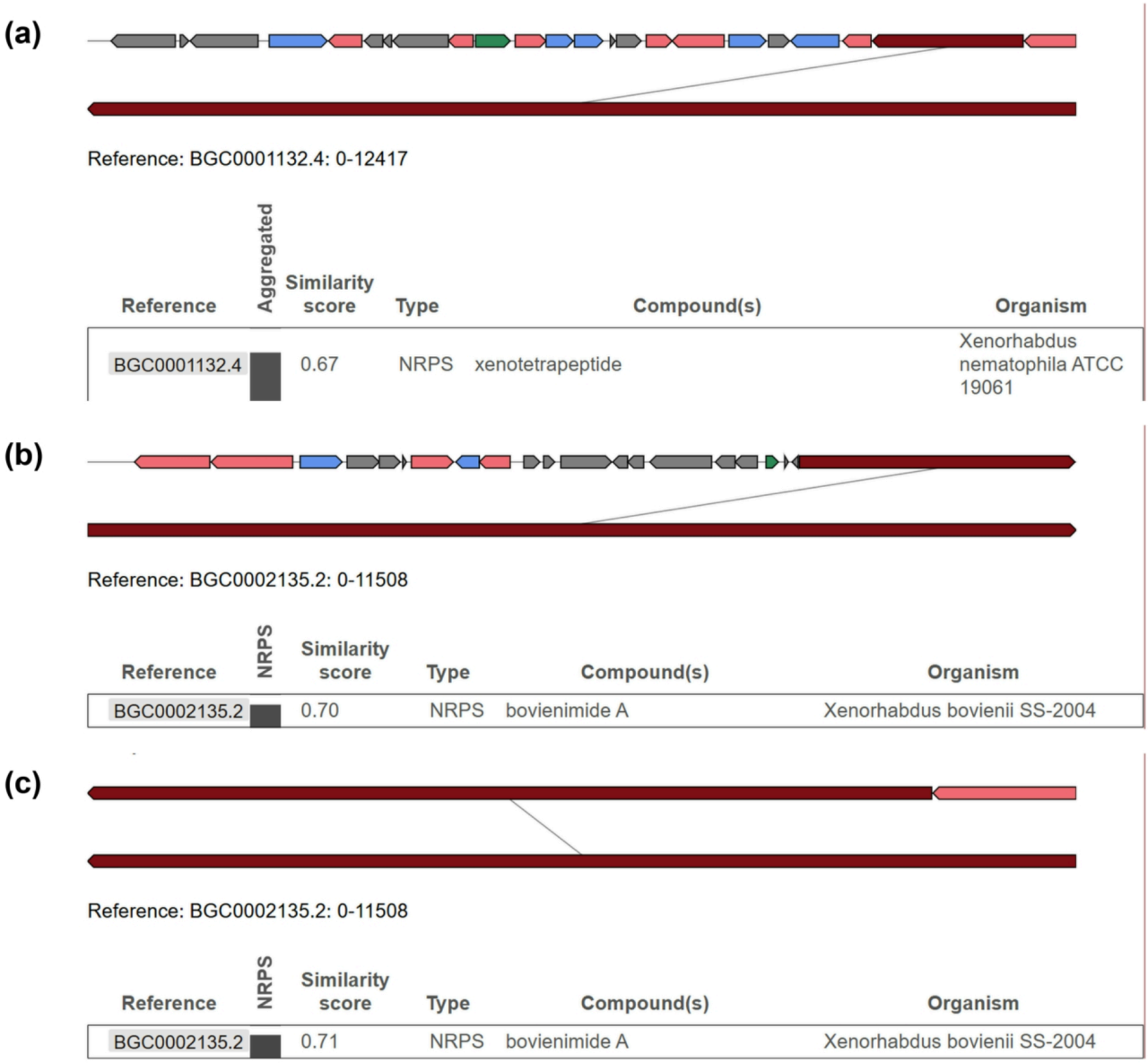


Figure 4

Comparative genomic organization and synteny of the identified BGCs. (a) Region 5.1 compared with the xenotetrapeptide reference cluster. (b) Region 6.2 and (c) region 10.1 compared with the bovienimide A reference cluster.

Supplementary Files

This is a list of supplementary files associated with this preprint. Click to download.

- patykasupplementsbacillussubtilisonu1125.pdf